Title

Incineration-Generated Polyethylene Micro-Nanoplastics Increase Triglyceride Lipolysis and Absorption in an In Vitro Small Intestinal Epithelium Model

Journal

Environmental Science and Technology, 56(17)

ISSN

0013-936X

Authors

DeLoid, Glen M

Cao, Xiaoqiong

Coreas, Roxana

et al.

Publication Date

2022-09-06

DOI

10.1021/acs.est.2c03195

Peer reviewed

HHS Public Access

Author manuscript

Environ Sci Technol. Author manuscript; available in PMC 2023 September 06.

Published in final edited form as:

Environ Sci Technol. 2022 September 06; 56(17): 12288–12297. doi:10.1021/acs.est.2c03195.

Incineration-generated polyethylene micro-nanoplastics (MNPs) increase triglyceride lipolysis and absorption in an *in vitro* small intestinal epithelium model

Glen M DeLoid[a,b,†], **Xiaoqiong Cao**[b,†], **Roxana Coreas**[c], **Dimitrios Bitounis**[a,b], **Dilpreet Singh**[a,b], **Wenwan Zhong**[c,d], **Philip Demokritou**[a,b,c,*]

[a.]Nanoscience and Advanced Materials Center, Environmental and Occupational Health Sciences Institute (EOHSI) and School of Public Health, Rutgers University, Piscataway, NJ 08854, USA

[b.]Center for Nanotechnology and Nanotoxicology, Department of Environmental Health, Harvard T. H. Chan School of Public Health, Boston, MA 02115, USA

[c.]Environmental Toxicology Graduate Program, University of California, Riverside, CA 92521, USA

[d.]Department of Chemistry, University of California, Riverside, CA 92521, USA

Abstract

Despite mounting evidence of micro-nanoplastics (MNPs) in food and drinking water, little is known of the potential health risks of ingested MNPs, and nothing is known of their potential impact on nutrient digestion and absorption. We assessed the effects of environmentally relevant secondary MNPs generated by incineration of polyethylene (PE-I), on digestion and absorption of fat in a high fat food model using a 3-phase *in vitro* simulated digestion coupled with a tri-culture small intestinal epithelium model. The presence of 400 μg/mL PE-I increased fat digestion by 33% and increased fat absorption by 147% and 145% 1 h and 2 h after exposure. Analysis of the PE-I lipid corona during digestion revealed predominantly triacylglycerols with enrichment of fatty acids in the small intestinal phase. Protein corona analysis showed enrichment of triacylglycerol lipase and depletion of β-casein in the small intestinal phase. These findings suggest digestion of triacylglycerol by lipase on the surface of lipid-coated MNPs as a potential mechanism. Further studies are needed to investigate the mechanisms underlying the greater observed increase in fat absorption, to verify these results in an animal model, and to determine the MNP properties governing their effects on lipid digestion and absorption.

Graphical Abstract

[*]Corresponding author: Philip Demokritou, philip.democritou@rugters.edu.

[†] These authors contributed equally to this work

Supporting Information

Supplementary methods; INEXS incineration platform schematic (Figure S1); Results of toxicity assessment of PE-I digesta exposures in the triculture model (Figure S2); Results of epithelial permeability assessment in PE-I digesta exposed triculture model (Figure S3); Schematic of intestinal fat digestion and absorption mechanisms (Figure S4)

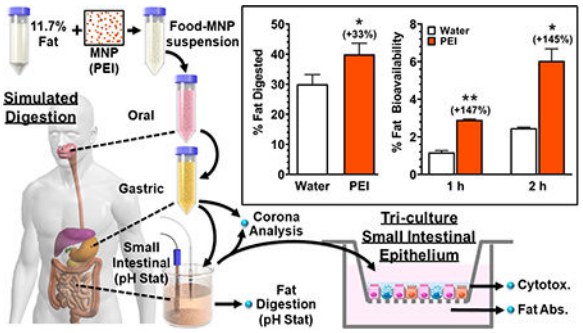

Keywords

plastics; incineration; microplastics; nanoplastics; micro-nanoplastics; polyethylene; ingestion; fat digestion; fat absorption

Introduction

The versatility, durability, and low cost of synthetic polymers (plastics) have rendered them indispensable and ubiquitous in modern society. Global annual production of plastic resins and fibers increased from two million metric tons (Mt) in 1950 to 380 million Mt in 2015[1,2]. As of 2015, an estimated 5.8 billion Mt of plastic waste had been generated, of which only about nine percent was recycled and twelve percent incinerated, while the remaining 79% was deposited in landfills and natural environments[1].

The impacts of plastic waste on marine wildlife and ecosystems have been recognized for years. Recently however, a more insidious potential hazard of plastic waste has emerged, namely micro-nanoplastics (MNPs), plastic particles and fibers produced by degradation and fragmentation of plastic waste. MNPs can be grouped into two broad categories: 1) primary MNPs: beads produced as abrasives for air-blasting, and until recently in personal care products, and 2) secondary MNPs created through fragmentation of plastic debris over time. Exposure of plastics to sunlight, water, and oxygen causes photo-oxidative degradation of the polymers[3]. This, combined with mechanical forces and thermal stress in the environment leads to fragmentation and generation of MNPs[1,4,5]. Secondary MNPs are also generated through thermal decomposition during incineration of plastic waste[6,7], and other industrial and commercial processes, including laser and 3D printing and photocopying, which generate airborne printer-emitted particles from polymer-based toners[8–10]. Secondary MNPs also enter freshwater from runoff from landfill, litter, and agricultural plastic, and deposition of airborne MNPs[4,6,11]. Recent studies have reported significant MNP contamination in terrestrial and freshwater environments, with some lake and river samples containing over 10^5 MNPs/m[3,5,12]. There is also evidence that MNPs can enter the food chain, through either direct ingestion of contaminated water or food, or trophic transfer[13].

By one estimate, humans ingest ~5 g of MNPs (one credit card) of plastics per week from food and beverages[14]. Little is yet known about the health implications of MNP ingestion, but a body of concerning evidence is growing. We recently reported size-dependent uptake and translocation of fluorescent carboxylated polystyrene (PS) MNPs,

accompanied by impaired barrier function (increased permeability), in an *in vitro* small intestinal epithelium model[15]. Other studies showed that PS MNPs were taken up by the GI tract in mice and rats[16–20]. More recently, MNPs were found in maternal and fetal zones of human placentas[21], suggesting potential maternal-fetal transfer, and translocation and deposition of 20 nm PS spheres in maternal organs and fetal tissues following intratracheal instillation in pregnant rats[22]. MNPs of multiple plastic polymers have also been found in human feces[23,24] and in human colectomy samples[25]. Most recently, pyrolysis – gas chromatography/mass spectrometry (Py-GCMS) analysis of blood from human volunteers revealed MNPs of four highly produced polymers (polyethylene (PE), Polyethylene terephthalate (PET), polystyrene (PS), and polymethyl methacrylate (PMMA)), with a mean total blood MNP concentration of 1.6 ± 2.3 μg/mL.[26]

With growing evidence of environmental, food, and drinking water contamination, access to the circulation, and widespread biodistribution of MNPs mounting fast, there is an urgent need to understand the health implications of MNP ingestion. While evaluation of toxicity in the GI tract, blood, and other tissues is essential, potential impacts of ingested MNPs on digestion and absorption of nutrients should not be overlooked. Studies from our lab and others have revealed significant impacts on digestion and uptake of nutrients resulting from co-ingestion of nanoscale materials, which have large specific surface areas and surface chemistries that enable interactions with digestive molecules and nutrients to impede or facilitate digestion of macronutrients to their bioaccessible forms, and with intestinal epithelial cells to alter nutrient absorption. The presence of ingested cellulose nanofibrils (CNF) in a high fat food model reduced lipolysis of triacylglycerides (TAG) to free fatty acids (FA) during *in vitro* simulated digestion as well as absorption of TAG in an *in vitro* small intestinal epithelium model by about half, and reduced serum TAG in rats after gavage with the high fat food model by about one third. These effects were driven primarily by coalescence of fat droplets on CNF, reducing the available surface area for lipase binding.[27] Studies from our lab and others have also reported significant effects of ingested nanoscale biopolymers such as cellulose and chitosan materials on carbohydrate digestion and absorption.[28–32] We have also found that ingested biopolymer nanomaterials and TiO_2 nanoparticles reduced zinc retention in mice,[33] and that both TiO_2 and SiO_2 nanoparticles increased *in vitro* absorption of a co-ingested pesticide, boscalid, partly through cell junction gene downregulation.[34,35]

Because many plastic polymers are hydrophobic, we hypothesized that MNPs could interact with fat and with membrane lipids and proteins to modulate digestion and/or absorption of fat. We further hypothesized that hydrophobic MNPs could adsorb fat, providing additional surface area for lipase binding and digestion. Finally, since we recently established that hydrophobic nanoscale PS MNPs readily enter enterocytes in an *in vitro* intestinal epithelium,[15] we hypothesized that fat-coated MNPs could facilitate absorption of fat by delivering fatty acids either to the cytoplasm or to the unstirred water layer. In this study we utilized an environmentally relevant secondary MNP, the $PM_{0.1}$ fraction of polyethylene MNPs (PE-I $PM_{0.1}$) generated by incineration using an incineration platform developed by the authors.[6,11] A 3-phase simulated digestion was used to measure hydrolysis of TAG (bioaccessibility) in a high fat food model, and an *in vitro* triculture small intestinal epithelium model was used to measure TAG absorption (bioavailability) from the small

intestinal digesta with and without PE-I. Finally, lipid and protein corona analysis of the PE-I MNPs before and after small intestinal digestion was performed to assess the potential role of lipid sorption to the MNPs in fat digestion and absorption.

Materials and methods

Study design.

An overview of the study design is shown in Figure 1. PE-I $PM_{0.1}$ MNPs were produced using the Integrated Exposure Generation (INEX) platform (see below for details). Dispersions of PE-I $PM_{0.1}$ MNPs were prepared in a high fat (11.7%) food model consisting of a mixture of commercially available heavy cream and a standardized food model previously described by the authors.[36] The dispersions were subjected to 3-phase simulated digestion to reproduce the transformations (surface chemistry changes, biocorona, agglomeration) that would occur *in vivo* prior to interactions of ingested MNPs with the intestinal epithelium, which is essential for producing physiologically relevant exposures that account for food matrix and gastrointestinal effects.[37] The extent of TAG lipolysis and FA production during the small intestinal phase was determined using pH Stat titration to monitor the amount of NaOH titrant required to maintain a pH of 7.0. The resulting small intestinal phase digestas were applied to the apical compartment of an *in vitro* transwell triculture small intestinal epithelial model including cells representing intestinal enterocytes (Caco-2), mucus secreting goblet cells (HT29-MTX), and microfold or M-cells (Caco-2 cells transformed by Raji B feeder cells).[38] Absorption of fat was assessed by measuring basolateral TAG and FA concentration one and two hours after exposure. Lipid and protein coronas of the PE-I MNPs were analyzed in the gastric and small intestinal digestas using the methods previously developed by the authors.[39]

Selection of starting MNP concentration in food model.

Due to the lack of accurate exposure data in emerging studies resulting from challenges measuring MNP particles smaller than several microns, relevant environmental water and food concentrations for MNPs are unclear. Estimates of MNPs released from plastic tea bags[40] and bottled water samples[41] range from about 0.2 to 10 μg/mL. On the other hand, a recent analysis estimated that humans consume an average of 5 g of MNPs per week, primarily through drinking water[14]. Assuming an average fluid and solid food intake of 3.0 L/d[42], this would correspond to an average MNP concentration in food and water consumed of ~240 μg/mL. For this study we chose a starting food concentration of 400 μg/mL, which because of the four-fold dilution of final digestas required to maintain adequate nutrition in the *in vitro* epithelium during exposure, corresponds to an oral concentration of 100 μg/mL. Given the continued exponential growth of plastic waste generation, and the likelihood that studies to date, typically with > 1 um detection limits, underestimate total MNP exposures, we believe this dose is justified.

Synthesis and dispersion of secondary MNPs: incinerated polyethylene particles.

Incinerated polyethylene (PE) MNP particles (PE-I) were generated by thermal decomposition of bulk-size PE pellets using our previously described Integrated Exposure Generation System (INEXS) (Figure S1), a versatile and reproducible platform to investigate

thermal decomposition behavior of materials under controlled combustion conditions, as previously described in detail.[6,11,43–46] Details are provided in supplementary materials.

High Fat food model.

A standardized food model (SFM), based on the average American diet, was recently developed and characterized in detail.[36] The SFM is prepared as an oil-in-water emulsion consisting of 3.4% protein (sodium caseinate), 4.6% sugar (sucrose), 5.2% digestible carbohydrate (corn starch), 0.7% dietary fiber (pectin), 3.4% fat (corn oil), and 0.5% sodium chloride. To prepare the high fat food model (HFFM) for this study, SFM was combined with heavy cream (33.3% fat, purchased from a local grocery store), water, and the stock PE-I $PM_{0.1}$ suspension and vortexed for 30 seconds to produce a final food model consisting of 11.7% fat, 1.7% protein, 2.3% sugar, 2.6% starch, 0.35% pectin, and 0.25% sodium chloride; with or without 400 μg/mL of PE-I $PM_{0.1}$

In vitro simulated digestion.

In vitro simulated digestion was performed using a 3-phase simulator as previously described.[38] Additional details are provided in supplementary materials.

Triculture small intestinal epithelial model.

The methods for generating the triculture model were previously described by the authors.[38] (Details are also provided in supplementary materials).

Exposure of triculture cellular model to digestas of food model with and without PE-I $PM_{0.1}$.

The final digestas of food model with and without PE-I $PM_{0.1}$ were combined with DMEM media in a ratio of 1:3, and the mixture was applied to cells (1.5 mL to the apical compartment for transwells, 200 μL per well for 96-well plates). Apical fluid in untreated control wells was replaced with fresh media. At 1 and 2 h 100 μL of basolateral fluid was collected for quantification of fat (TAG and FA) translocation (fat absorption). Additionally, at 24 h transepithelial electrical resistance (TEER) in transwells was measured, and apical fluid from transwells was collected for LDH analysis. Analysis of ROS production was performed after 6 h exposure of cells in 96-well plates, and cell viability and apoptosis were assessed at 24 h in 96-well plates. Finally, assessment of the triculture monolayer permeability to dextran was performed 3 h after exposure to provide an assessment of effects on passive transcellular and paracellular transport shortly after the last measurements to assess fat absorption.

Cytotoxicity (LDH release) assessment.

Release of LDH was measured using the Pierce LDH assay kit (Sigma Aldrich, St. Louis, MO) as previously described by the authors.[15,38] Details are provided in supplementary materials.

Measurement of reactive oxygen species (ROS) production.

Production of ROS was assessed in cells grown and treated in 96-well plates using the CellROX® green reagent (Thermo Fisher, Waltham MA). Briefly, a 5 mM working solution of CellROX® green was prepared from 20 mM stock by diluting in DMEM media without FBS. Media was removed from test wells and replaced with 100 μL working solution. Plates were incubated at 37 °C for 30 minutes. Wells were washed 3 times with 200 μL PBS, and fluorescence was measured at 480 nm (excitation)/520 nm (emission).

Cell viability (mitochondrial metabolic activity).

Cell viability was assessed using the PrestoBlue™ reagent (Thermo Inc., Waltham, MA) as previously described.[15,38] Details are provided in supplementary materials.

Apoptosis (Caspase 3/7 activity) measurement.

Apoptosis was assessed in 96-well plates after 24 h exposures using the CellEvent Caspase-3/7 Green Detection kit (ThermoFisher). Details of the method are provided in supplementary materials.

Epithelial permeability measurement using fluorescent dextran.

Fluorescently labeled dextrans of two sizes and colors (Alexa Fluor 488 3 kDa and Texas Red 70 kDa, Thermo Inc., Waltham, MA) were diluted in PSB to 25 μg/mL each. After 3 h exposure to digestas, cells were washed twice with PBS and 2 mL of the dextran solution was applied to the apical compartment while 2 mL of fresh DMEM without phenol red or FBS was added to the basolateral compartment. After incubation of cells at 37 °C for 60 min, 0.3 mL samples of basolateral fluids were obtained and fluorescence was measured for both dextrans (Ex 495 nm, Em 519 nm for Alexa Fluor 488 3 kDa dextran and Ex 595, Em 615 for Texas Red 70 kDa dextran) using a SpectraMax M-5 microplate reader and SoftMax Pro acquisition and analysis software (Molecular Devices, San Jose, CA).

Measurement of free FA and TG in basolateral fluid samples.

Free FA concentrations in basolateral fluid samples were measured using a fluorometric assay kit (Cayman Chemical, Ann Arbor, MI), and TG was measured using a colorimetric assay kit (Cayman Chemical) according to the manufacturer's protocols.

Lipid and protein corona extraction.

Methods for lipid and protein corona extraction are provided in supplementary materials and described by the authors in their previous publication.[39]

Proteomic and lipidomic analysis.

Methods used for proteomic and lipidomic analysis are provided in supplementary materials and described by the authors in their previous publication.[39]

Statistical analysis.

Cytotoxicity and fat absorption experiments were performed in triplicate. Six replicates were included in simulated digestion experiments. Statistical analysis was performed and

graphs were prepared using Prism 9.3.1 software (GraphPad Software, Inc., San Diego, CA). Results of toxicological assays, pH stat digestions, basolateral TAG and FA data, and fat bioavailability were analyzed using an unpaired *t* test with Welch's correction. Protein and lipid abundances were normalized using total ion abundances with the former restricted to peptide spectrum matches >1. Relative abundances were analyzed using student's *t* test to interpret *p*-values and enrichment was calculated using $\log_2$ fold changes of abundances using Excel and plotted with Prism 9.3.1.

Results

Physicochemical characterization of PE-I PM 0.1.

Detailed physicochemical and morphological characterization of PE-I particles was published previously.[6,44] In summary, PE-I consisted of mostly organic carbonaceous compounds (99.7% w/w) and 0.3% w/w elemental carbon. Particles contained appreciable amounts of low and high molecular weight polycyclic aromatic hydrocarbons (PAH) (72.5 μg/g).

Colloidal characterization of PE-I $PM_{0.1}$ dispersion in water.

Characterization of the water dispersion of PE-I PM0.1 MNP was previously reported by our lab.[46] Dynamic light scattering (DLS) analysis revealed a monomodal distribution with a mean hydrodynamic diameter (d_H) of 528.7 ± 16.4 nm and a polydispersity index (PdI) of 0.35 ± 0.08. The zeta potential (ζ) and conductance (σ) measured by Electrophoretic light scattering (ELS) were −14.5 ± 0.9 mV and 0.011 ± 0.57 mS/cm, respectively.

In vitro toxicity of ingested PE-I MNPs in the triculture model.

Exposure of the *in vitro* triculture small intestinal epithelium to small intestinal digestas of HFFM containing PE-I $PM_{0.1}$ at a final concentration of 8.33 μg/mL (from starting 400 μg/mL in HFFM) had no significant effects on epithelial health compared to digesta of HFFM alone (Figure S2). Transepithelial electrical resistance (TEER) after 24 h exposure was above the 1000 Ω cm^2 value at which the triculture epithelial barrier is considered to be intact (Figure S2 a). Cytotoxicity, measured after 24 h exposure by LDH release, was below 5% (Figure S2 b), within the normal range of 5–10%. Cell viability at 24 h, measured with the PrestoBlue assay, an indicator of metabolic activity, was slightly but not significantly decreased in the presence of MNPs (84 ± 7%) compared to wells treated with digestas of HFFM alone (98 ± 4%) (Figure S2 c). Finally, PE-I had no effect on production of reactive oxygen species (ROS), measured at 6 h (Figure S2 d), and likewise had no significant effect on caspase 3/7 activity, an indicator of apoptosis, measured at 24 h.

Effect of ingested PE-I MNPs on epithelial permeability in the triculture model.

Exposure of the triculture epithelium to small intestinal digestas of HFFM containing PE-I $PM_{0.1}$ had no significant effect on permeability to either 3 kDa or 70 kDa fluorescently labeled dextran (Figure S3). No differences were observed in basolateral fluid fluorescence for either 3 kDa (green fluorescent) or 70 kDa (red fluorescent) dextran between digestas with or without MNPs. While 3 kDa dextran permeability may reflect changes in either paracellular permeability or fluid-phase transcytosis, 70 kDa permeability is specific for

paracellular diffusion. The observed absence of changes indicate that PE-I had no effect on either transcytosis or paracellular transport.

Effects of ingested PE-I on lipolysis during simulated digestion.

Because lipolysis generates free fatty acids (FA) and hydrogen ions (H^+), the amount of titrant (NaOH) added during the small intestine phase to maintain the pH at 7.0, measured by pH-Stat titration, can be used to determine the total amount of FA/ H^+ released, and thus the extent of TAG lipolysis. The percentages of total fat hydrolyzed during the small intestinal phase of *in vitro* simulated digestion of HFFM with and without PE-I are shown in Figure 2 a. The presence of PE-I increased lipolysis by 33% over HFMM alone, from 29% of total available fat hydrolyzed in HFFM alone to 39% in HFFM with PE-I ($N=6$, $p<0.05$).

Effects on fat bioavailability.

In the presence of PE-I basolateral concentrations and total masses of both TAG (Figure 2 b) and FA (Figure 2 c) as well as the corresponding percentages of applied fat absorbed (Figure 2 d) were all more than twice the corresponding values for absorption from digestas of HFFM. Specifically, PE-I increased cumulative TAG absorption by 207% at 1 h and by 137% at 2 h, and increased FA absorption by 112% at 1 h and 160% at 2h. Overall fat absorption (sum of basolateral TAG and FA masses as a percentage of total mass of fat applied) was increased in the presence of PE-I by 147% and 145% at 1 h and 2 h, respectively.

Composition of the lipid corona of ingested PE-I after gastric and small intestinal digestion of HFFM.

Lipid compositions extracted from gastric and small intestinal digestas of HFFM without PE-I, as well as PE-I lipid corona digestas (HFFM containing 0.4 mg/mL PE-I), are represented as pie charts in Figure 3. In the gastric phase digesta of HFFM, most of the lipid was TAG (93.44%), with a smaller percentage of DAG (6.05%), and negligible amounts of FA, ceramides, and sterols (Figure 3 a). Following small intestinal digestion, the TAG component of the HFFM digesta was partially depleted (80.15%), accompanied by relative enrichment of DAG (13.21%), FA (3.0%), and sterols (3.04%) (Figure 3 b). The depletion of TAG and enrichment of DAG and FA are expected as a result of pancreatic TAG lipase activity, while enrichment of sterols was likely due to bile salts (cholesterol derivatives) added to the small intestinal digestion. The composition of the PE-I lipid corona in the gastric phase of the HFFM with PE-I was similar to the gastric phase HFFM only lipid profile, but with a smaller fraction of TAG (89.75%), and larger fractions of FA (1.46%) and DAG (7.55%) (Figure 3 c). At the end of small intestinal digestion (Figure 3 d), as with the HFFM only digesta, the TAG component of the PE-I corona was depleted (82.96%). However, unlike the HFFM only digesta profile, there was only a slight enrichment of DAG (8.43%) in the PE-I corona, and a greater enrichment of FA (6.33%) relative to the gastric phase corona, indicating more extensive digestion of PE-I corona lipids than of lipids in the HFFM only digesta.

Composition of the protein corona of ingested PE-I after gastric and small intestinal digestion of HFFM.

Comparisons of proteins identified in gastric and small intestinal digestas of HFFM alone and in coronas of PE-I from gastric and small intestinal digestas of HFFM in the presence of PE-I are summarized in Figure 4. Enrichment or depletion of identified proteins in the PE-I corona of gastric phase relative to small intestinal phase digestas of HFFM in the presence of PE-I are represented as volcano plots (log10 p-value vs. log2 fold change) in Figure 4 a. Enrichment or depletion in gastric phase PE-I corona compared to the gastric phase digesta of HFFM alone, and in small intestinal phase PE-I corona compared to small intestinal digesta of HFFM alone are shown in Figure 4 b and c. A total of 72 identified proteins were significantly ($p<0.5$) enriched or depleted in one or more of the three volcano plot comparisons. These proteins are listed with enrichment/depletion in each comparison represented as a heatmap in Figure 4 d. The greatest differences were seen between gastric and intestinal phase PE-I coronas. Among the few proteins depleted in the gastric phase PE-I corona compared to the small intestinal phase PE-I corona (i.e., enriched in the intestinal phase PE-I corona), the most notable is triacylglycerol lipase, the enzyme that carries out lipolysis of TAG, normally on the surface of lipid droplets. Several proteins were strongly enriched in the gastric vs. small intestinal PE-I corona (i.e., depleted in the small intestinal PE-I corona). The most notable of these was β-casein, which normally coats and stabilizes milk fat globules, and is displaced by bile salts during fat digestion to provide greater surface area for lipase binding and activity. The depletion of β-casein and enrichment of TAG lipase in the small intestinal phase PE-I corona is consistent with digestion of lipids on the surface of PE-I by the same mechanism that occurs on fat droplets.

Discussion and Conclusions

In *in vitro* simulated digestions of a high fat (11.7%) food model we observed that 0.4 mg/mL PE-I MNPs increased lipolysis of TAGs during the small intestinal phase by 33% (Figure 2 a) and more than double the amount of TAG and FA absorbed in an *in vitro* small intestinal epithelium model (Figure 2 b and c), increasing total fat absorption by nearly 2.5 fold, far more than would be expected to result from the 33% increase in digestion alone. Exposure to digestas of HFFM containing PE-I caused no significant toxicity (Figure S2) and did not alter permeability to either 3 kDa or 70 kDa dextran (Figure S3), and therefore had no effect on either transcytosis or paracellular transport, ruling out the possibility that cell health or altered permeability contributed to the observed increase.

Analysis of the lipid coronas of PE-I in gastric and small intestinal phase digestas (Figure 3 c and d) revealed predominantly TAG, with FA relatively enriched after small intestinal digestion (from 1.46% in gastric phase to 6.33% in small intestinal phase). Notably, enrichment of FA in small intestinal vs. gastric digestas of HFFM alone was less pronounced (3.0% in small intestinal phase). These findings suggest that TAGs are adsorbed onto the surfaces of PE-I MNPs and digested on the surface of lipid-coated PE-I particles, analogous to normal lipolysis on fat globule surfaces. This is in line with the 33% increase in fat digestion observed during simulated digestions (Figure 2 a). The results of protein corona analysis of PE-I (Figure 4) provide further evidence of this: the enzyme triacylglycerol

lipase, responsible for most TAG digestion on lipid droplet surfaces, was strongly enriched (5.08-fold) in the small intestinal vs. gastric phase PE-I corona, consistent with binding of lipase to the MNP lipid corona. Moreover, β-casein, which normally coats milk fat droplets until displaced during by bile salts to enable lipase binding, was markedly depleted (9.36-fold) in the small intestinal PE-I corona.

Together, these data suggest that the observed increase in TAG digestion in the presence of PE-I MNPs could in part be due to additional surface area for lipase binding provided by lipid coated MNPs. However, if this mechanism is to account for a 33% increase in digestion, the surface area provided by the lipid-coated MNPs should be sufficient to substantially increase the surface area of the fat droplets present. While we cannot, without further studies alluded to above, definitively state that PE-I augmented lipolysis by increasing the available surface area for lipase binding, the PE-I lipid and protein corona findings are strongly suggestive of this mechanism.

Finally, the observed 2.5-fold increase in fat absorption cannot be fully accounted for by the observed 1.33-fold increase in fat digestion and proportional increase in free FA and MAG present in the digestas. Without further studies and a more detailed understanding of the process and regulation of fat absorption, we can only speculate as to how the presence of PE-I MNPs accelerated this process so substantially. We can, however, rule out a few possibilities: First, because permeability to 3 kDa and 70 kDa dextran was unaffected by exposure to PE-I digestas (Figure S3), we can rule out any role of paracellular permeability or fluid phase transcytosis. Second, since the increase was observed within one hour of exposure, and it takes on average one hour to transcribe and translate a protein[47], we can rule out the possibility that a changes in expression of proteins involved in uptake, trafficking, or processing of fat played a significant role. What remains when these possibilities are excluded are direct biophysical and biochemical interactions between the PE-I MNPs and the molecules and processes involved in lipid uptake.

Our current understanding of the process of fat (TAG) absorption, reviewed by Thomson et al.,[48] Pan and Hussain,[49] and Demignot et al.,[50] is illustrated in Figure S4 a. Briefly, lipase binds to lipid droplets, assisted by bile salts. Lipolysis products, FA and monoacylglycerols (MAG), are incorporated into mixed-micelles coated with bile salts. Whereas free FA and MAG cannot enter the unstirred water layer (UWL) to reach the apical membrane, mixed micelles are able to enter the UWL, where an acidic microclimate facilitates dissociation and release of free FA and MAG. Uptake of FAs beings with interaction of the FA with the outer plasma membrane monolayer, followed by a “flip-flop” of the bilayer, and finally, intracellular delivery of the FA. Several membrane proteins are thought to be involved in the transport of FAs into enterocytes, including CD36/FAT2 (fatty acid translocase 2), plasma membrane fatty acid binding protein ($FABP_{pm}$), and fatty acid transport protein 4 (FATP4), although their specific roles are not well understood. Uptake is also facilitated by intracellular acyl-CoA synthase 1, which acylates FAs with CoA, trapping them within the cytosol and activating them for TAG re-synthesis in the endoplasmic reticulum (ER). Cytosolic FA-CoAs are transported to the ER by acyl-CoA FA binding proteins (ACBP), while MAG enters by diffusion. Within the ER, TAGs are regenerated from MAGs and FA-CoAs in a two-step process by the enzymes monoacylglycerol:acylCoA acyltransferase

2 (MGAT2), and diacylglycerol:acylCoA acyltransferase 1 (DGAT1). The TAGs produced in the ER are packaged by microsomal TAG transfer protein (MTP) into prechylomicrons (PC). the PCs are transported in PC transport vesicles (PCTV) to the *cis* golgi, where ApoA1 is added to generate the mature chylomicrons (CM), which are transported to the *trans* golgi, and subsequently exit trans golgi in membrane bound vesicles that fuse with the basolateral enterocyte membrane, secreting the CMs into the basolateral lamina propria. It is important to note that during lipid absorption, in addition to producing chylomicrons, enterocytes transiently store lipid in lipid droplets (LD) within the cytosol. The dynamic redistribution of TAGs between the ER and LD storage can affect the overall rate of lipid secretion.

We can only speculate as to how PE-I MNPs increased the uptake, processing, and/or secretion of TAGs (Figure S4 b). However, since we have shown that the digested PE-I MNPs possessed a lipid corona composed of TAGs and FAs, one possibility might be that PE-I particles directly transported lipids either into the UWL or into the cytoplasm. In our recent study we showed that hydrophobic PS MNPs entered caco-2 enterocytes in the same triculture cellular system. Additional studies are needed to determine whether PE-I is capable of entering either the UWL, where the acidic microenvironment might facilitate release of FAs from their surfaces or crossing the plasma membrane and delivering FAs to the cytoplasm. Another potential mechanism might involve delivery of activated FAs (FA-CoAs) and MAGs to the ER for TAG resynthesis, delivering both substrates directly to MGAT2, which could decrease the effective K_m for the enzyme and increase the rate of DAG synthesis. Finally, a shift of the dynamic balance between cytosolic and LD lipid toward the cytoplasm could accelerate chylomicron production and secretion.

Given the ongoing human ingestion exposures to MNPs and the global epidemic of obesity and its many comorbidities, the possibility that such exposures could increase absorption of ingested fat is concerning. By changing the amount or composition of lipids entering the colon, the altered digestion and absorption of fat caused by ingested PE-I could also impact the gut microbiome. A high fat diet has been shown to rapidly and reversibly alter the gut microbiota in mice,[51,52] and is frequently used to induce obesity, typically accompanied by gut dysbiosis, in experimental animals.[52–54] As summarized in recent reviews, although interventional changes in dietary fat have not been found to consistently alter the gut microbiome composition in humans, several observational studies have reported an inverse correlation between fat intake and gut microbiota diversity in humans.[52,55,56] Moreover, gut dysbiosis has been implicated in neuro-psychiatric disorders that often accompany obesity, which are thought to be mediated by the activity of the gut microbiota through the “microbiota-gut-brain axis”, recently reviewed by Cryan et al.[57] and Morais et al..[58] Reduced lipid delivery to the colon due to increased absorption in the presence of PE-I might therefore improve the diversity of the gut microbiome and thereby ameliorate these disorders.

Further studies are needed to determine whether or not PE-I MNPs or other hydrophobic MNPs can cause the observed increase in lipid digestion by providing additional surface area for lipase binding, and to identify the mechanisms responsible for the greater increase in lipid absorption in the presence of PE-I. Additional studies are also needed to assess the effects of ingested PE-I on fat digestion in a normal or low fat diet and determine the

extent to which the observed increases in fat digestion and absorption caused by PE-I are dependent upon a high dietary fat content. In addition, animal studies are needed to assess whether these *in vitro* findings translate to meaningful effects in a whole animal. Such studies should include evaluation of effects of MNP-induced changes in fat digestion and absorption on the microbiota in those animals as discussed above. Finally, while PE is one of the most highly produced of the major plastic polymers, there are several other highly produced polymers with widely varied chemistries, and the effects of their MNPs on nutrient digestion and absorption should be assessed separately for each polymer.

Supplementary Material

Refer to Web version on PubMed Central for supplementary material.

Acknowledgements

Support for the research reported was provided by the National Institute of Environmental Health Sciences of the National Institutes of Health under Award Number (NIH grant # U24ES026946) as part of the Nanotechnology Health Implications Research (NHIR) Consortium. R. C. was supported by the Research Training Grant in Environmental Toxicology from the NIEHS (Award # T32ES026946). Lipidomics/proteomics were conducted at the Integrative Genome Biology Core at the University of California Riverside supported in part by NIH S10 OD010669. The content is solely the responsibility of the authors and does not necessarily represent the official view of the National Institutes of Health. Funding was also provided by the Rutgers NIEHS Center for Environmental Exposure and Diseases (CEED) (Award # P30 ES005022)

References

(1). Geyer R; Jambeck JR; Law KL Production, Use, and Fate of All Plastics Ever Made. Sci. Adv 2017, 3 (7). 10.1126/sciadv.1700782.

(2). Plastics-the Facts 2018 An analysis of European plastics production, demand and waste data https://plasticseurope.org/wp-content/uploads/2021/10/2018-Plastics-the-facts.pdf (accessed 2022 -08 -04).

(3). Gewert B; Plassmann MM; Macleod M Pathways for Degradation of Plastic Polymers Floating in the Marine Environment. Environmental Sciences: Processes and Impacts. Royal Society of Chemistry September 1, 2015, pp 1513–1521. 10.1039/c5em00207a.

(4). Horton AA; Walton A; Spurgeon DJ; Lahive E; Svendsen C Microplastics in Freshwater and Terrestrial Environments: Evaluating the Current Understanding to Identify the Knowledge Gaps and Future Research Priorities. Science of the Total Environment. Elsevier B.V. May 2017, pp 127–141. 10.1016/j.scitotenv.2017.01.190.

(5). Shahul Hamid F; Bhatti MS; Anuar N; Anuar N; Mohan P; Periathamby A Worldwide Distribution and Abundance of Microplastic: How Dire Is the Situation? Waste Management and Research. SAGE Publications Ltd October 2018, pp 873–897. 10.1177/0734242X18785730.

(6). Sotiriou GA; Singh D; Zhang F; Chalbot M-CG; Spielman-Sun E; Hoering L; Kavouras IG; Lowry GV; Wohlleben W; Demokritou P Thermal Decomposition of Nano-Enabled Thermoplastics: Possible Environmental Health and Safety Implications. J. Hazard. Mater 2016, 305, 87–95. 10.1016/j.jhazmat.2015.11.001. [PubMed: 26642449]

(7). Froggett SJ; Clancy SF; Boverhof DR; Canady RA A Review and Perspective of Existing Research on the Release of Nanomaterials from Solid Nanocomposites. Part. Fibre Toxicol 2014, 11, 17. 10.1186/1743-8977-11-17. [PubMed: 24708765]

(8). Pirela SV; Martin J; Bello D; Demokritou P Nanoparticle Exposures from Nano-Enabled Toner-Based Printing Equipment and Human Health: State of Science and Future Research Needs. Crit. Rev. Toxicol 2017, 47 (8). 10.1080/10408444.2017.1318354.

(9). Pirela SVSV; Pyrgiotakis G; Bello D; Thomas T; Castranova V; Demokritou P Development and Characterization of an Exposure Platform Suitable for Physico-Chemical, Morphological and

Toxicological Characterization of Printer-Emitted Particles (PEPs). Inhal. Toxicol 2014, 26 (7), 400–408. 10.3109/08958378.2014.908987. [PubMed: 24862974]

(10). Pirela S; Molina R; Watson C; Cohen JM; Bello D; Demokritou P; Brain J Effects of Copy Center Particles on the Lungs: A Toxicological Characterization Using a Balb/c Mouse Model. Inhal. Toxicol 2013, 25 (9), 498–508. 10.3109/08958378.2013.806614. [PubMed: 23895351]

(11). Sotiriou GA; Singh D; Zhang F; Wohlleben W; Chalbot M-CG; Kavouras IG; Demokritou P An Integrated Methodology for the Assessment of Environmental Health Implications during Thermal Decomposition of Nano-Enabled Products. Environ. Sci. Nano 2015, 2 (3), 262–272. 10.1039/C4EN00210E. [PubMed: 26200119]

(12). Moore CJ; Lattin GL; Zellers AF Quantity and Type of Plastic Debris Flowing from Two Urban Rivers to Coastal Waters and Beaches of Southern California. Rev. Gestão Costeira Integr. 2011, 11 (1), 65–73. 10.5894/rgci194.

(13). Toussaint B; Raffael B; Angers-Loustau A; Gilliland D; Kestens V; Petrillo M; Rio-Echevarria IM; Van den Eede G Review of Micro- and Nanoplastic Contamination in the Food Chain. Food Additives and Contaminants - Part A Chemistry, Analysis, Control, Exposure and Risk Assessment. Taylor and Francis Ltd. May 2019, pp 639–673. 10.1080/19440049.2019.1583381.

(14). Wit W. de; Bigaud N No Plastic in Nature: Assessing Plastic Ingestion from Nature to People; WWF - World Wide Fund for Nature: Gland, Switzerland, 2019.

(15). DeLoid GM; Cao X; Bitounis D; Singh D; Llopis PM; Buckley B; Demokritou P Toxicity, Uptake, and Nuclear Translocation of Ingested Micro-Nanoplastics in an in Vitro Model of the Small Intestinal Epithelium. Food Chem. Toxicol 2021, 158, 112609. 10.1016/J.FCT.2021.112609. [PubMed: 34673181]

(16). Walczak AP; Kramer E; Hendriksen PJM; Tromp P; Helsper JPFG; Van Der Zande M; Rietjens IMCM; Bouwmeester H Translocation of Differently Sized and Charged Polystyrene Nanoparticles in in Vitro Intestinal Cell Models of Increasing Complexity. Nanotoxicology 2015, 9 (4), 453–461. 10.3109/17435390.2014.944599. [PubMed: 25093449]

(17). Jani P; Halbert GW; Langridge J; Florence AT The Uptake and Translocation of Latex Nanospheres and Microspheres after Oral Administration to Rats. J. Pharm. Pharmacol 1989, 41 (12), 809–812. 10.1111/j.2042-7158.1989.tb06377.x. [PubMed: 2576440]

(18). Jani PU; McCarthy DE; Florence AT Nanosphere and Microsphere Uptake via Peyer's Patches: Observation of the Rate of Uptake in the Rat after a Single Oral Dose. Int. J. Pharm 1992, 86 (2–3), 239–246. 10.1016/0378-5173(92)90202-D.

(19). Deng Y; Zhang Y; Lemos B; Ren H Tissue Accumulation of Microplastics in Mice and Biomarker Responses Suggest Widespread Health Risks of Exposure. Sci. Rep 2017, 7 (1), 1–10. 10.1038/srep46687. [PubMed: 28127051]

(20). Liang B; Zhong Y; Huang Y; Lin X; Liu J; Lin L; Hu M; Jiang J; Dai M; Wang B; Zhang B; Meng H; Lelaka JJJ; Sui H; Yang X; Huang Z Underestimated Health Risks: Polystyrene Micro- and Nanoplastics Jointly Induce Intestinal Barrier Dysfunction by ROS-Mediated Epithelial Cell Apoptosis. Part. Fibre Toxicol 2021, 18 (1), 20. 10.1186/s12989-021-00414-1. [PubMed: 34098985]

(21). Ragusa A; Svelato A; Santacroce C; Catalano P; Notarstefano V; Carnevali O; Papa F; Rongioletti MCA; Baiocco F; Draghi S; D'Amore E; Rinaldo D; Matta M; Giorgini E Plasticenta: First Evidence of Microplastics in Human Placenta. Environment International. Elsevier Ltd January 1, 2021, p 106274. 10.1016/j.envint.2020.106274.

(22). Fournier SB; D'Errico JN; Adler DS; Kollontzi S; Goedken MJ; Fabris L; Yurkow EJ; Stapleton PA Nanopolystyrene Translocation and Fetal Deposition after Acute Lung Exposure during Late-Stage Pregnancy. Part. Fibre Toxicol 2020, 17 (1). 10.1186/S12989-020-00385-9.

(23). Schwabl P; Koppel S; Konigshofer P; Bucsics T; Trauner M; Reiberger T; Liebmann B Detection of Various Microplastics in Human Stool: A Prospective Case Series. Ann. Intern. Med 2019, 171 (7), 453–457. 10.7326/M19-0618/SUPPL_FILE/M19-0618_SUPPLEMENT.PDF. [PubMed: 31476765]

(24). Zhang N; Li Y. Bin; He HR; Zhang JF; Ma GS You Are What You Eat: Microplastics in the Feces of Young Men Living in Beijing. Sci. Total Environ 2021, 767, 144345. 10.1016/J.SCITOTENV.2020.144345. [PubMed: 33434834]

(25). Ibrahim YS; Tuan Anuar S; Azmi AA; Wan Mohd Khalik WMA; Lehata S; Hamzah SR; Ismail D; Ma ZF; Dzulkarnaen A; Zakaria Z; Mustaffa N; Tuan Sharif SE; Lee YY Detection of Microplastics in Human Colectomy Specimens. JGH Open 2021, 5 (1), 116–121. 10.1002/JGH3.12457. [PubMed: 33490620]

(26). Leslie HA; van Velzen MJM; Brandsma SH; Vethaak AD; Garcia-Vallejo JJ; Lamoree MH Discovery and Quantification of Plastic Particle Pollution in Human Blood. Environ. Int 2022, 107199. 10.1016/J.ENVINT.2022.107199. [PubMed: 35367073]

(27). Deloid GM; Sohal IS; Lorente LR; Molina RM; Pyrgiotakis G; Stevanovic A; Zhang R; McClements DJ; Geitner NK; Bousfield DW; Ng KW; Loo SCJ; Bell DC; Brain J; Demokritou P Reducing Intestinal Digestion and Absorption of Fat Using a Nature-Derived Biopolymer: Interference of Triglyceride Hydrolysis by Nanocellulose. ACS Nano 2018, 12 (7), 6469–6479. 10.1021/acsnano.8b03074. [PubMed: 29874029]

(28). Liu L; Kong F The Behavior of Nanocellulose in Gastrointestinal Tract and Its Influence on Food Digestion. J. Food Eng 2021, 292, 110346. 10.1016/j.jfoodeng.2020.110346.

(29). Nsor-Atindana J; Douglas Goff H; Liu W; Chen M; Zhong F The Resilience of Nanocrystalline Cellulose Viscosity to Simulated Digestive Processes and Its Influence on Glucose Diffusion. Carbohydr. Polym 2018, 200, 436–445. 10.1016/j.carbpol.2018.07.088. [PubMed: 30177185]

(30). Ji N; Liu C; Li M; Sun Q; Xiong L Interaction of Cellulose Nanocrystals and Amylase: Its Influence on Enzyme Activity and Resistant Starch Content. Food Chem. 2018, 245, 481–487. 10.1016/j.foodchem.2017.10.130. [PubMed: 29287399]

(31). Liu L; Kerr WL; Kong F; Dee DR; Lin M Influence of Nano-Fibrillated Cellulose (NFC) on Starch Digestion and Glucose Absorption. Carbohydr. Polym 2018, 196, 146–153. 10.1016/j.carbpol.2018.04.116. [PubMed: 29891281]

(32). Guo Z; DeLoid GM; Cao X; Bitounis D; Sampathkumar K; Ng KW; Loo SCJ; Demokritou P Effects of Ingested Nanocellulose and Nanochitosan Materials on Carbohydrate Digestion and Absorption in an in Vitro Small Intestinal Epithelium Model. Environ. Sci. Nano 2021, 8 (9), 2554–2568. 10.1039/D1EN00233C. [PubMed: 34840801]

(33). Gonçalves JP; Pipek LZ; Donaghey TC; DeLoid GM; Demokritou P; Brain JD; Molina RM Effects of Ingested Nanomaterials on Tissue Distribution of Co-Ingested Zinc and Iron in Normal and Zinc-Deficient Mice. NanoImpact 2021, 21. 10.1016/J.IMPACT.2020.100279.

(34). Cao X; Khare S; Deloid GM; Gokulan K; Demokritou P Co-Exposure to Boscalid and TiO2 (E171) or SiO2 (E551) Downregulates Cell Junction Gene Expression in Small Intestinal Epithelium Tricultures and Increases Pesticide Translocation. Nanoimpact 2021, 22, 1–8.

(35). Cao X; DeLoid GM; Bitounis D; De La Torre-Roche R; White JC; Zhang Z; Ho CG; Ng KW; Eitzer BD; Demokritou P Co-Exposure to the Food Additives SiO 2 (E551) or TiO 2 (E171) and the Pesticide Boscalid Increases Cytotoxicity and Bioavailability of the Pesticide in a Tri-Culture Small Intestinal Epithelium Model: Potential Health Implications . Environ. Sci. Nano 2019, 6 (9), 2786–2800. 10.1039/c9en00676a. [PubMed: 32133147]

(36). Zhang Z; Zhang R; Xiao H; Bhattacharya K; Bitounis D; Demokritou P; McClements DJ Development of a Standardized Food Model for Studying the Impact of Food Matrix Effects on the Gastrointestinal Fate and Toxicity of Ingested Nanomaterials. NanoImpact 2019, 13, 13–25. 10.1016/J.IMPACT.2018.11.002. [PubMed: 31093583]

(37). McClements DJ; DeLoid G; Pyrgiotakis G; Shatkin JA; Xiao H; Demokritou P The Role of the Food Matrix and Gastrointestinal Tract in the Assessment of Biological Properties of Ingested Engineered Nanomaterials (IENMs): State of the Science and Knowledge Gaps. NanoImpact 2016, 3–4, 47–57. 10.1016/j.impact.2016.10.002.

(38). DeLoid GM; Wang Y; Kapronezai K; Lorente LR; Zhang R; Pyrgiotakis G; Konduru NV; Ericsson M; White JC; De La Torre-Roche R; Xiao H; McClements DJ; Demokritou P An Integrated Methodology for Assessing the Impact of Food Matrix and Gastrointestinal Effects on the Biokinetics and Cellular Toxicity of Ingested Engineered Nanomaterials. Part. Fibre Toxicol 2017, 14 (1), 40. 10.1186/s12989-017-0221-5. [PubMed: 29029643]

(39). Coreas R; Cao X; DeLoid GM; Demokritou P; Zhong W Lipid and Protein Corona of Food-Grade TiO2 Nanoparticles in Simulated Gastrointestinal Digestion. NanoImpact 2020, 20. 10.1016/j.impact.2020.100272.

(40). Hernandez LM; Xu EG; Larsson HCE; Tahara R; Maisuria VB; Tufenkji N Plastic Teabags Release Billions of Microparticles and Nanoparticles into Tea. Environ. Sci. Technol 2019. 10.1021/acs.est.9b02540.

(41). Koelmans AA; Mohamed Nor NH; Hermsen E; Kooi M; Mintenig SM; De France J Microplastics in Freshwaters and Drinking Water: Critical Review and Assessment of Data Quality. Water Research. Elsevier Ltd May 15, 2019, pp 410–422. 10.1016/j.watres.2019.02.054.

(42). Costanzo LS; Preceded by: Costanzo LS Physiology, 6th ed.; Elservier, 2017.

(43). Pal AKAK; Watson CYCY; Pirela SVSV; Singh D; Chalbot M-CGM-CG; Kavouras I; Demokritou P Linking Exposures of Particles Released From Nano-Enabled Products to Toxicology: An Integrated Methodology for Particle Sampling, Extraction, Dispersion, and Dosing. Toxicol. Sci 2015, 146 (2), 321–333. 10.1093/toxsci/kfv095. [PubMed: 25997654]

(44). Singh D; Schifman LA; Watson-Wright C; Sotiriou GA; Oyanedel-Craver V; Wohlleben W; Demokritou P Nanofiller Presence Enhances Polycyclic Aromatic Hydrocarbon (PAH) Profile on Nanoparticles Released during Thermal Decomposition of Nano-Enabled Thermoplastics: Potential Environmental Health Implications. Environ. Sci. Technol 2017, 51 (9), 5222–5232. 10.1021/ACS.EST.6B06448. [PubMed: 28397486]

(45). Singh D; Marrocco A; Wohlleben W; Park HR; Diwadkar AR; Himes BE; Lu Q; Christiani DC; Demokritou P Release of Particulate Matter from Nano-Enabled Building Materials (NEBMs) across Their Lifecycle: Potential Occupational Health and Safety Implications. J. Hazard. Mater 2022, 422. 10.1016/J.JHAZMAT.2021.126771.

(46). Watson-Wright C; Singh D; Demokritou P Toxicological Implications of Released Particulate Matter during Thermal Decomposition of Nano-Enabled Thermoplastics. NanoImpact 2017, 5, 29–40. 10.1016/J.IMPACT.2016.12.003. [PubMed: 29333505]

(47). Milo R; Phillips R Cell Biology by the Numbers, 17th ed.; CRC Press: Boca Raton, FL, 2015.

(48). Thomson ABR; Schoeller C; Keelan M; Smith L; Clandinin MT Lipid Absorption: Passing through the Unstirred Layers, Brush-Border Membrane, and Beyond. Can. J. Physiol. Pharmacol 1993, 71 (8), 531–555. 10.1139/Y93-078. [PubMed: 8306192]

(49). Pan X; Hussain MM Gut Triglyceride Production. Biochim. Biophys. Acta 2012, 1821 (5), 727–735. 10.1016/J.BBALIP.2011.09.013. [PubMed: 21989069]

(50). Demignot S; Beilstein F; Morel E Triglyceride-Rich Lipoproteins and Cytosolic Lipid Droplets in Enterocytes: Key Players in Intestinal Physiology and Metabolic Disorders. Biochimie 2014, 96 (1), 48–55. 10.1016/J.BIOCHI.2013.07.009. [PubMed: 23871915]

(51). Yun E-J; Imdad S; Jang J; Park J; So B; Kim J-H; Kang C Diet Is a Stronger Covariate than Exercise in Determining Gut Microbial Richness and Diversity. Nutrients 2022, 14 (12), 2507. 10.3390/NU14122507. [PubMed: 35745235]

(52). Gérard P The Crosstalk between the Gut Microbiota and Lipids. OCL 2020, 27, 70. 10.1051/OCL/2020070.

(53). Safari Z; Bruneau A; Monnoye M; Mariadassou M; Philippe C; Zatloukal K; Gérard P Murine Genetic Background Overcomes Gut Microbiota Changes to Explain Metabolic Response to High-Fat Diet. Nutrients 2020, 12 (2). 10.3390/NU12020287.

(54). Busnelli M; Manzini S; Jablaoui A; Bruneau A; Kriaa A; Philippe C; Arnaboldi F; Colombo A; Ferrari B; Ambrogi F; Maguin E; Rhimi M; Chiesa G; Gérard P Fat-Shaped Microbiota Affects Lipid Metabolism, Liver Steatosis, and Intestinal Homeostasis in Mice Fed a Low-Protein Diet. Mol. Nutr. Food Res 2020, 64 (15), 1900835. 10.1002/MNFR.201900835.

(55). Wolters M; Ahrens J; Romaní-Pérez M; Watkins C; Sanz Y; Benítez-Páez A; Stanton C; Günther K Dietary Fat, the Gut Microbiota, and Metabolic Health - A Systematic Review Conducted within the MyNewGut Project. Clin. Nutr 2019, 38 (6), 2504–2520. 10.1016/J.CLNU.2018.12.024. [PubMed: 30655101]

(56). Mokkala K; Houttu N; Cansev T; Laitinen K Interactions of Dietary Fat with the Gut Microbiota: Evaluation of Mechanisms and Metabolic Consequences. Clin. Nutr 2020, 39 (4), 994–1018. 10.1016/J.CLNU.2019.05.003. [PubMed: 31171289]

(57). Cryan JF; O'riordan KJ; Cowan CSM; Sandhu KV; Bastiaanssen TFS; Boehme M; Codagnone MG; Cussotto S; Fulling C; Golubeva AV; Guzzetta KE; Jaggar M; Long-Smith CM; Lyte JM; Martin JA; Molinero-Perez A; Moloney G; Morelli E; Morillas E; O'connor R; Cruz-Pereira

JS; Peterson VL; Rea K; Ritz NL; Sherwin E; Spichak S; Teichman EM; van de Wouw M; Ventura-Silva AP; Wallace-Fitzsimons SE; Hyland N; Clarke G; Dinan TG The Microbiota-Gut-Brain Axis. Physiol. Rev 2019, 99 (4), 1877–2013. 10.1152/PHYSREV.00018.2018. [PubMed: 31460832]

(58). Morais LH; Schreiber HL; Mazmanian SK The Gut Microbiota–Brain Axis in Behaviour and Brain Disorders. Nat. Rev. Microbiol 2020 194 2020, 19 (4), 241–255. 10.1038/s41579-020-00460-0. [PubMed: 33093662]

Synopsis

An *in vitro* study of the effects of ingestion of an environmentally relevant micro-nanoplastic (MNP), nanoscale particles generated by incineration of polyethylene (PE-I), revealed that the presence of MNPs can increase fat digestion and absorption, underscoring the need for further studies to evaluate potential interactions of MNPs, an important emerging contaminant in the environment, food, and drinking water, with the digestion and uptake of nutrients.

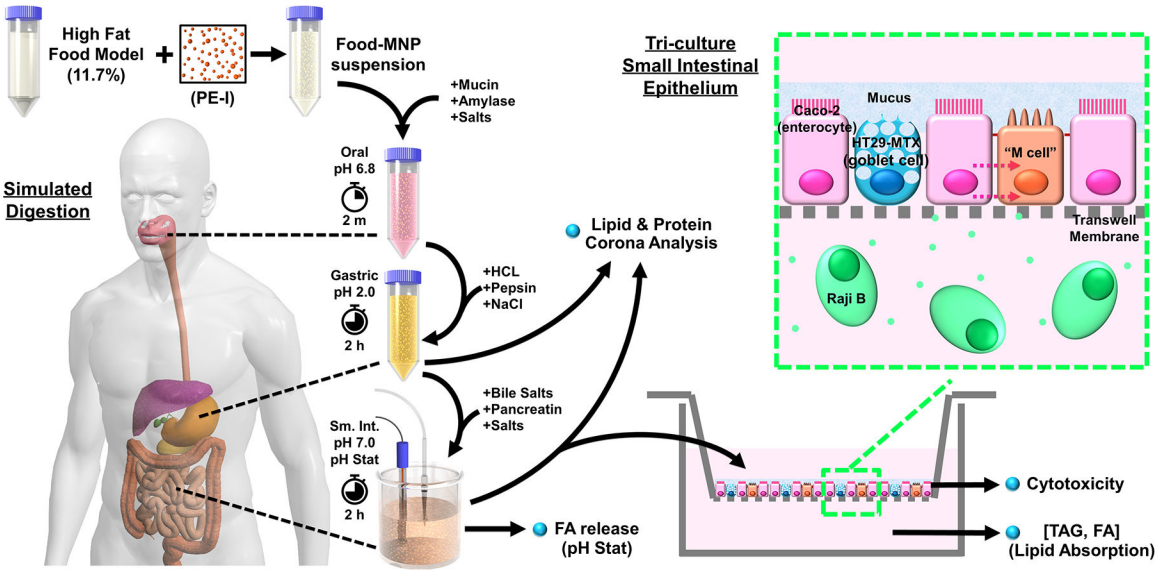

Figure 1.
Study design overview.

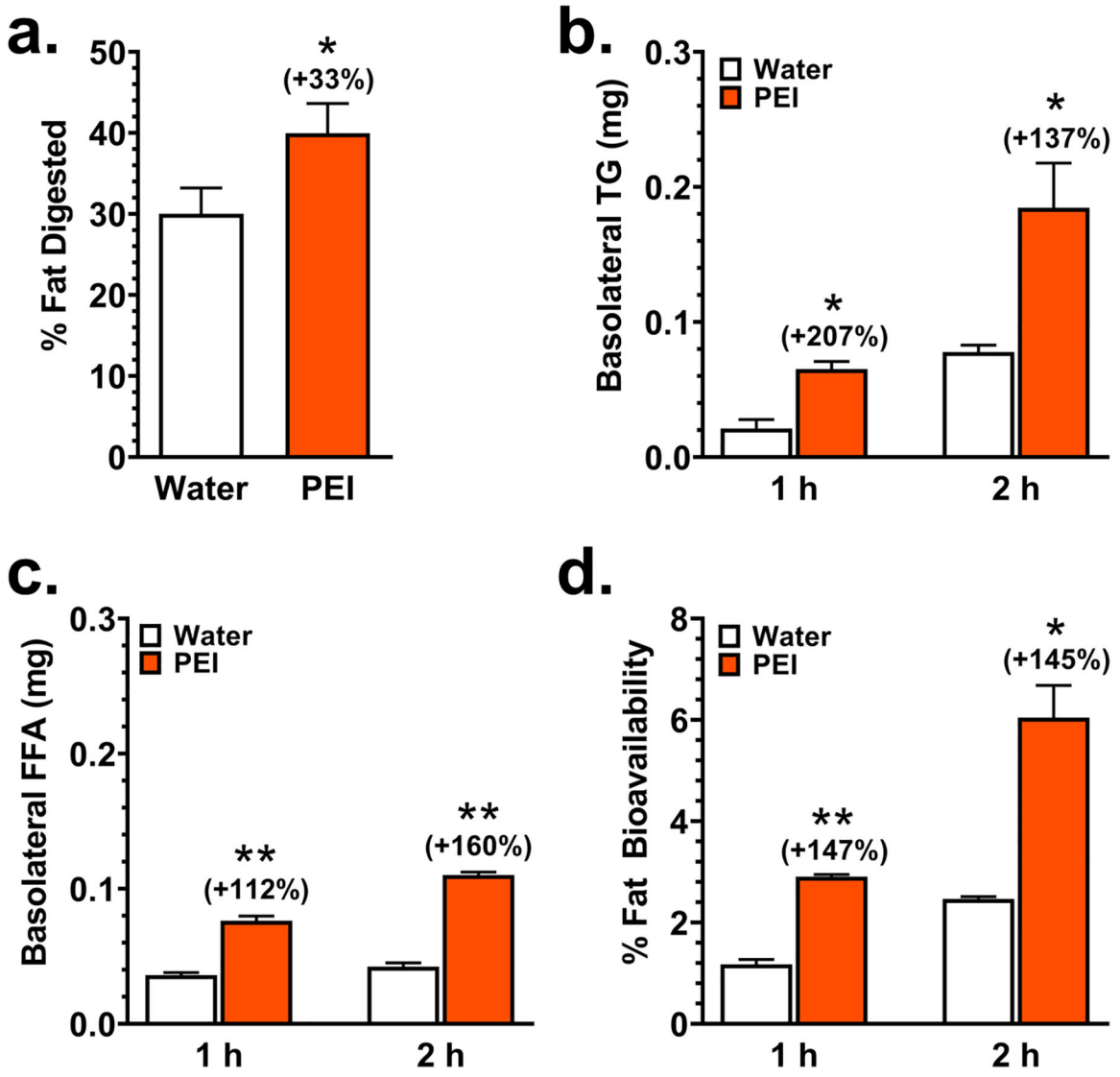

Figure 2. Effect of ingested PE-I on lipid digestion and absorption.

HFFM with and without 0.4 mg/mL PE-I was subjected to 3-phase simulated digestion, with pH stat titration during the small intestinal phase for quantification of lipolysis. Digestas were applied to triculture transwells and FA and TAG in the basolateral compartment were measured at 1 and 2 h to assess fat absorption. **a.** Percent of fat digested based on amount of NaOH titrant consumed (measured by pH stat titration) to maintain a constant pH of 7.0 during small intestinal digesta, **b.** Mass of TAG in the basolateral compartment 1 h and 2 h after applying digesta to cells in the apical compartment, **c.** Mass of FFA in basolateral compartment 1 h and 2 h after applying digesta to the apical compartment, **d.** Percentages of applied fat in basolateral compartment (TG + FFA) 1 h and 2 h after application of digestas to cells. N=3. PE-I: Incinerated Polyethylene, $PM_{0.1}$ fraction. * $p < 0.05$. ** $p < 0.01$.

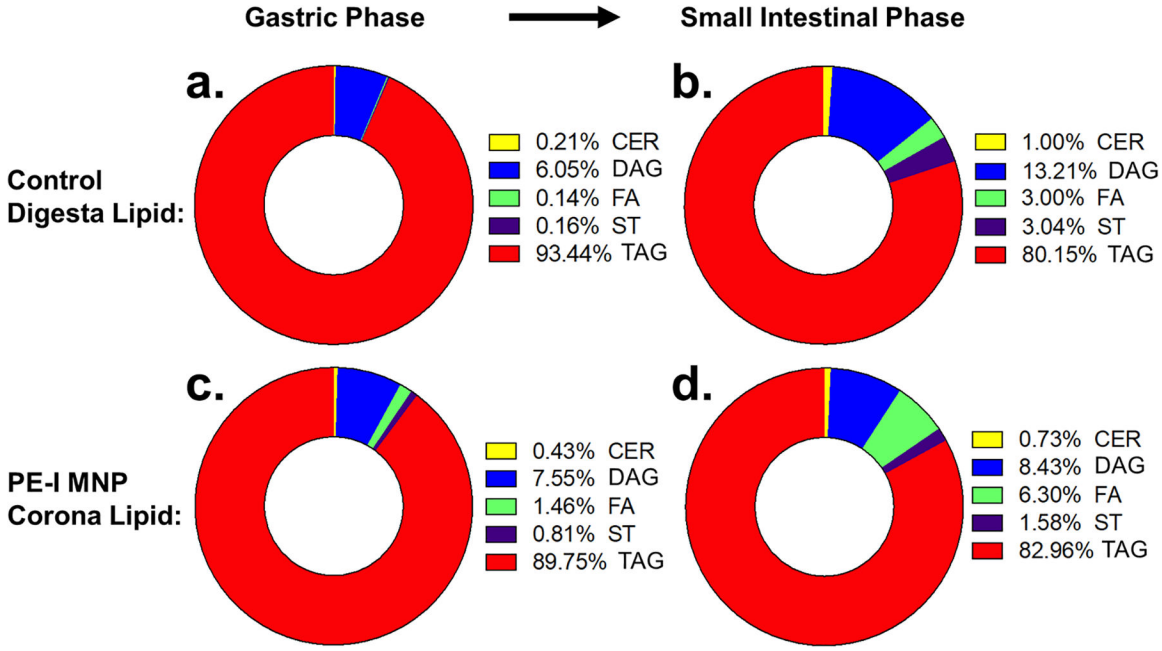

Figure 3. Analysis of lipids in HFFM digesta and PE-I coronas before and after lipid digestion.

a. Lipid profile of gastric phase digesta of HFFM alone. **b.** Lipid profile of small intestinal digesta of HFFM alone. **c.** Lipid profile of PE-I lipid corona after gastric phase digestion of HFFM in the presence of PE-I. **d.** Lipid profile of PE-I lipid corona after small intestinal phase digestion of HFFM in the presence of PE-I. PE-I: Incinerated Polyethylene, $PM_{0.1}$ fraction; CER: ceramides; DAG: diacylglycerides; FA: fatty acids; ST: sterols; TAG: triacylglycerides.

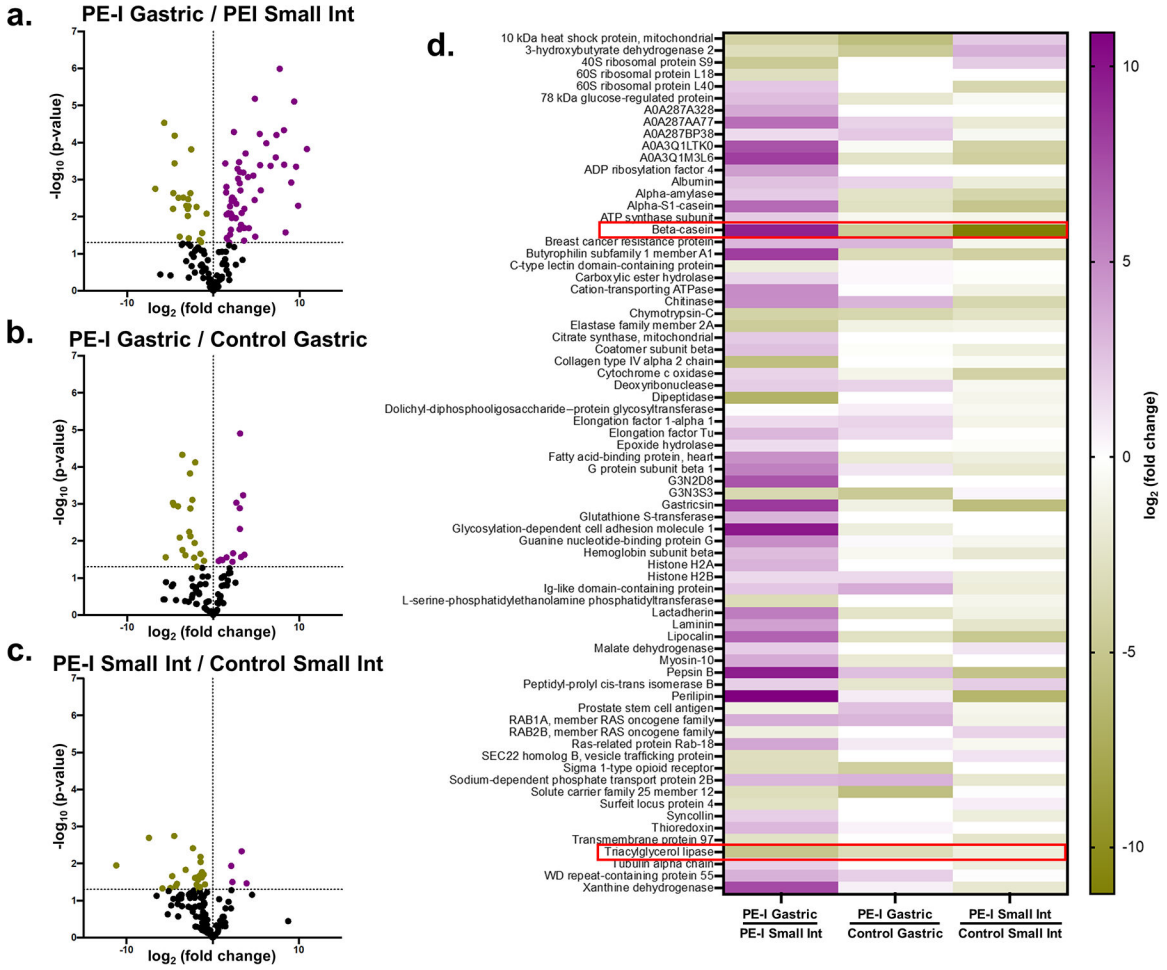

Figure 4. Analysis of proteins in HFFM digesta and PE-I coronas after gastric and small intestinal digestion.

a. Volcano plot (log10 p-value vs. log2 fold change) for identified proteins in the PE-I corona in gastric phase digestas relative to small intestinal phase digestas of HFFM + PE-I. **b.** Volcano plot for identified proteins in the gastric phase PE-I corona (from digestion of HFFM + PE-I) relative to the gastric phase digesta of HFFM alone. **c.** Volcano plot for identified proteins in the small intestinal phase PE-I corona (from digestion of HFFM + PE-I) relative to the small intestinal phase digesta of HFFM alone. **d.** Heatmap of log2 fold changes for significantly enriched or depleted proteins from the three volcano plots in a-c.